Journal of Archaeological Science: Reports 46 (2022) 103723

Contents lists available at ScienceDirect

Journal of Archaeological Science: Reports

journal homepage: www.elsevier.com/locate/jasrep

Combining quantitative approaches to differentiate between backed products from discoidal and Levallois reduction sequences

Guillermo Bustos-Pérez [a,b,c,*], Brad Gravina [d,e], Michel Brenet [e,f], Francesca Romagnoli [a,*]

[a] Departamento de Prehistoria y Arqueología, Universidad Autónoma de Madrid, Campus de Cantoblanco, 28049 Madrid, Spain
[b] Institut Català de Paleoecologia Humana i Evolució Social (IPHES-CERCA), Zona Educacional 4, Campus Sescelades URV (Edifici W3), 43007 Tarragona, Spain
[c] Universitat Rovira i Virgili, Departament d'Història i Història de l'Art, Avinguda de Catalunya 35, 43002 Tarragona, Spain
[d] Musée national de Préhistoire, MC, 1 rue du Musée, 24260 Les Eyzies de Tayac, France
[e] Univ. Bordeaux, CNRS, MC, PACEA, UMR-5199, FF-33600 Pessac, France
[f] INRAP Grand Sud-Ouest, Centre mixte de recherches archéologiques, Domaine de Campagne, 242460 Campagne, France

ARTICLE INFO

Keywords:
Lithic analysis
Levallois
Discoid
Geometric morphometrics
Machine learning
Deep learning

ABSTRACT

Backed flakes (core edge flakes and pseudo-Levallois points) represent special products of Middle Paleolithic centripetal flaking strategies. Their peculiarities are due to their roles as both a technological objective and in the management of core convexities to retain its geometric properties during reduction. In Middle Paleolithic contexts, these backed implements are commonly produced during Levallois and discoidal reduction sequences. Backed products from Levallois and discoidal reduction sequences often show common geometric and morphological features that complicate their attribution to one of these methods. This study examines the identification of experimentally produced discoidal and recurrent centripetal Levallois backed products (including all stages of reduction) based on their morphological features. 3D geometric morphometrics are employed to quantify morphological variability among the experimental sample. Dimensionality reduction though principal component analysis is combined with 11 machine learning models for the identification of knapping methods. A supported vector machine with polynomial kernel has been identified as the best model (with a general accuracy of 0.76 and an area under the curve [AUC] of 0.8). This indicates that combining geometric morphometrics, principal component analysis, and machine learning models succeeds in capturing the morphological differences of backed products according to the knapping method.

1. Introduction

The Middle Paleolithic in Western Europe is characterized by the diversification of and an increase in knapping methods, resulting in flake-dominated assemblages (Kuhn, 2013; Delagnes and Meignen, 2006). Discoidal and the recurrent centripetal Levallois are two of the most common flake production systems during this period. Following Boëda (1995a,b, 1994, 1993), there are six technological criteria that define discoidal debitage: (1) the volume of the core is conceived as two oblique asymmetric convex surfaces delimited by an intersection plane; (2) these two surfaces are not hierarchical as they alternately serve as striking platforms and debitage surfaces; (3) the peripheral convexity of the debitage surface is managed to control lateral and distal removals, thus allowing for a degree of predetermination; (4) striking platforms are oriented in such a way that the core edge is perpendicular to the predetermined products; (5) the fracture planes are secant; and (6) the technique employed is direct hard-hammer percussion. Technological analyses of Middle Paleolithic assemblages have gradually led to the identification of variability within discoidal reduction (Bourguignon and Turq, 2003; Locht, 2003; Terradas, 2003; articles in Peresani, 2003).

In addition, according to Boëda (1994, 1993), six technological characteristics define the Levallois knapping strategy: (1) the volume of the core is conceived as two convex and asymmetric surfaces; (2) these two surfaces are hierarchical and are not interchangeable—they maintain their roles as peripheral striking platforms and debitage (or exploitation) surfaces, respectively, throughout the reduction sequence; (3) the distal and lateral convexities of the debitage surface are maintained to obtain predetermined flakes; (4) the fracture plane of the

* Corresponding authors at: Departamento de Prehistoria y Arqueología, Universidad Autónoma de Madrid, Campus de Cantoblanco, 28049 Madrid, Spain (Guillermo Bustos-Pérez).
E-mail addresses: guillermo.bustos@uam.es (G. Bustos-Pérez), francesca.romagnoli@uam.es (F. Romagnoli).

https://doi.org/10.1016/j.jasrep.2022.103723
Received 15 July 2022; Received in revised form 16 September 2022; Accepted 27 October 2022
Available online 5 November 2022

predetermined products is parallel to the intersection between both surfaces; (5) the striking platform is perpendicular to the overhang (the core edge at the intersection between the two core surfaces); and (6) the technique employed is direct hard-hammer percussion. Depending on the organization of the debitage surface, Levallois cores are usually classified into the preferential method (where a single predetermined Levallois flake is obtained from the debitage surface) and the recurrent method (where several predetermined flakes are produced from the debitage surface), with removals being either unidirectional, bidirectional, or centripetal (Boëda, 1995a,b; Boëda et al., 1990; Delagnes, 1995; Delagnes and Meignen, 2006).

Both knapping methods involve the removal of backed products (Fig. 1) that usually comprise two categories: core edge flakes (*éclats débordants*) and pseudo-Levallois points. Core edge flakes/*éclat débordant* (Beyries and Boëda, 1983; Boëda, 1993; Boëda et al., 1990) are technical backed knives that have a cutting edge opposite and parallel (or sub-parallel) to an abrupt margin (a back that usually has an angle close to 90°). This back commonly results from the removal of one of the lateral edges of the core and can be plain, retain the scars from previous removals, be cortical, or a combination of these attributes. Core edge flakes are also divided into two categories: "classic core edge flakes" and "core edge flakes with a limited back". "Classic core edge flakes" (Beyries and Boëda, 1983; Boëda, 1993; Boëda et al., 1990), which are sometimes referred to as "core edge flakes with a non-limited back"/*"éclat débordant à dos non limité"* (Duran, 2005; Duran and Soler, 2006), have a morphological axis more or less similar to the axis of percussion. "Core edge flakes with a limited back"/*"éclat débordant à dos limité"* have a offset axis of symmetry in relation to the axis of percussion (Meignen,1993, 1996; Pasty et al., 2004). This orientation often leads to the back not being parallel to nor spanning the entire length of the sharp edge or the percussion axis (Slimak, 2003).

Pseudo-Levallois points (Boëda, 1993; Boëda et al., 1990; Bordes, 1961, 1953; Slimak, 2003) are backed products where the edge opposite the back has a triangular morphology. This triangular morphology is usually the result of the convergence of two or more scars. As with core edge flakes, the back usually results from the removal of one of the lateral edges of the core and can be plain, retain the scars from previous removals, or more rarely be cortical or a combination of these traits. Both pseudo-Levallois points and core edge flakes with a limited back share a symmetry offset from the axis of percussion but are clearly differentiable due to their morphology. The present study includes the three categories defined above as backed products.

Depending on the knapping method, different roles in Levallois recurrent centripetal and discoidal debitage are attributed to core edge flakes and pseudo-Levallois points. Boëda et al. (1990) focus on the role of core edge flakes and cortically backed flakes for maintaining the lateral convexities throughout Levallois recurrent centripetal reduction. Similarly, pseudo-Levallois points contribute to maintaining the lateral and distal convexities between different series of removals (Boëda et al., 1990).

Focusing on the variability of discoidal debitage, Slimak (2003) noted that pseudo-Levallois points are short products that induce a limited lowering of the core overhang (the intersection between the striking and debitage surfaces). In contrast, core edge flakes can result from several distinct production objectives. Expanding on the roles of pseudo-Levallois points and core edge flakes within discoidal debitage, Locht (2003) demonstrated the systematic production of both products at the site of Beauvais. This indicates that at Beauvais, core edge flakes and pseudo-Levallois points were the main predetermining/predetermined products (Locht, 2003).

An additional aspect of core edge flakes and pseudo-Levallois points is their frequent transport by Paleolithic groups. Turq et al. (2013) described the widespread import and export of lithic artifacts during the Middle Paleolithic. Examples (Fig. 2) of the transport of pseudo-Levallois points from discoidal production sequences have been reported from Combemenue, La Mouline, Les Fieux (Brenet, 2013, 2012; Brenet and Cretin, 2008; Folgado and Brenet, 2010; Turq et al., 2013), and the open-air site of Bout des Vergnes (Courbin et al., 2020), while the transport of core edge flakes (into and out of the site) is also clearly observed at Grotte Vaufrey (Geneste, 1988), Teixoneres Cave (Bustos-Pérez et al., 2017; Picin et al., 2020), Amalda Cave (Rios-Garaizar, 2010), Grotta del Cavallo (Romagnoli et al., 2016a), l'Arbreda (Duran and Soler, 2006) and at Site N of Maastricht-Belvédère (Roebroeks et al., 1992). Transported backed pieces have also been clearly identified at Abric Romaní in Spain associated with both Levallois and discoidal reduction methods (Romagnoli et al., 2016b; Martín-Viveros et al., 2020). The identification of knapping methods among these specific products can help to indentify diachronic and synchronic changes in lithic production, selection, and transport as a reflection of hominin technological organization and adaptive strategies (Binford, 1979; Shott, 2018).

The attribution of backed pieces to either discoidal or recurrent centripetal Levallois reduction can, however, be problematic. For example, Mourre (2003) indicates that a key aspect for the identification of Levallois core edge flakes is the direction of the debitage axis, which is parallel to the intersection plane of the two core surfaces while the fracture plane is secant. Slimak (1998–99) showed core edge flakes from discoidal reduction to equally have fracture planes parallel to the intersection between the debitage surface and striking platforms although not as parallel as in Levallois debitage. Delpiano et al. (2021)

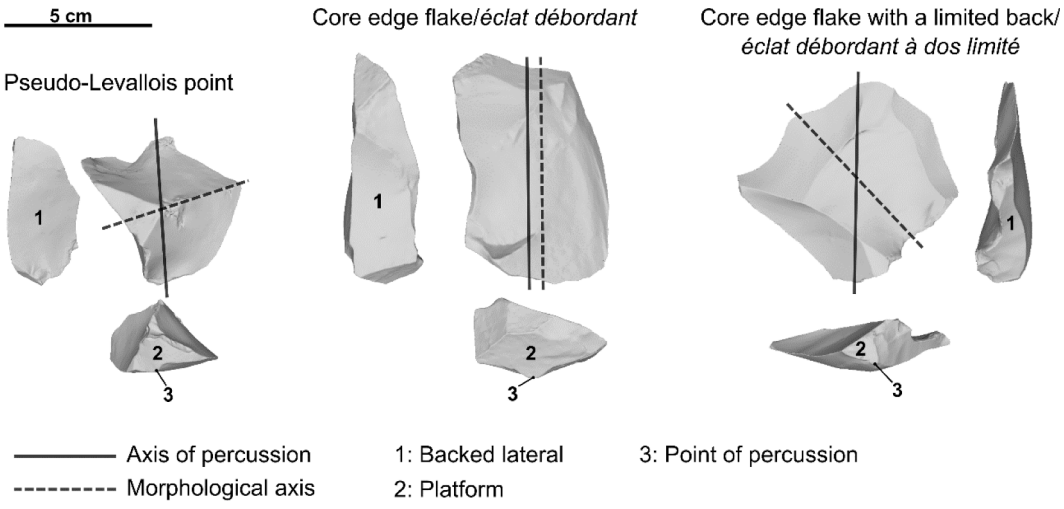

Fig. 1. Examples of backed flakes categories with key features discussed in the present research.

Fig. 2. Middle Paleolithic sites cited in the text showing examples of transport of backed products from discoidal or Levallois recurrent centripetal sequences (base map obtained from https://maps-for-free.com/).

demonstrated a tendency of Levallois products to be more elongated with thinner and sub-parallel edges, whereas discoidal backed products show a higher variation in the minimum and maximum thickness of the back. Previous studies (Archer et al., 2021; González-Molina et al., 2020) addressed the differentiation between discoidal and recurrent centripetal Levallois products in general terms were all products are considered. While this approach is highly effective, the differentiation between backed products of discoidal and recurrent centripetal Levallois sequences is not sufficiently addressed. Given the special technological role of backed products in core management and production, their specific techno-functional properties (Delpiano et al., 2021), the frequency in which they appear in the archaeological record, and their common transport as part of hominin toolkits, a more systematic approach to their accurate differentiation represents an important advancement in describing Middle Paleolithic lithic assemblages.

This raises the issue as to the extent to which discoidal and Levallois recurrent centripetal core edge flakes and pseudo-Levallois points can be differentiated based on their morphological features. This issue is relevant to lithic studies because it affects the technological analysis of a stone tool assemblage and the evolutionary interpretation of knapping concepts over time. Here we address this issue through experimental archaeology and a multi-level statistical approach. We reproduced classic bifacial discoidal and recurrent centripetal Levallois reduction sequences to obtain a collection of backed products. We produced 3D scans of lithic artifacts and employed geometric morphometrics to quantify the morphological variability of the experimental sample and the cores were refit. Dimensionality reduction through principal component analysis (PCA) was carried out on a set of coordinates, and 11 machine learning models were tested to obtain classification accuracy and variable importance. Geometric morphometrics and Machine Learning models make it possible to directly test technological classifications of lithic and features usually employed to discriminate between both methods.

2. Methods

2.1. Experimental assemblage

The analyzed experimental assemblage derives from the replication of nine discrete knapping sequences. Seven cores were knapped in Bergerac chert (Fernandes et al., 2012), and two cores were knapped in Miocene chert from South of Madrid (Bustillo et al., 2012; Bustillo and Pérez-Jiménez, 2005). Five cores were knapped following the discoidal *"sensu stricto"* method, which corresponds highly to Boëda's original technological definition of the knapping system (Boëda, 1993, 1994, 1995a,b), and five experimental cores were knapped following the Levallois recurrent centripetal system (Boëda, 1993, 1994, 1995a,b; Lenoir and Turq, 1995). A total of 139 unretouched backed flakes (independent of the type of termination) were obtained: 70 from the discoidal reduction sequences and 69 from the Levallois reduction sequences (Fig. 3). In the case of the Levallois recurrent centripetal cores, backed products from both debitage and striking surfaces were included.

The Levallois recurrent centripetal experimental assemblage is clearly dominated by non-cortical backed flakes (n = 42; 60.87 %; Fig. 2). This is expected as one of the roles of core edge flakes and pseudo-Levallois points in Levallois recurrent centripetal methods is the management of convexities on subsequent exploitation sequences (Boëda, 1993, 1994; Boëda et al., 1990). Thus, although backed flakes can be present in the initial decortication phases (n = 9; 13.04 %), the subsequent exploitation of the core will equally produce non-cortical flakes. Non-cortical backed flakes are also the majority class of the experimental discoidal assemblage although this predominance is somewhat attenuated (n = 29; 41.43 %; Fig. 2). However, along with flakes with nearly 25 % of the dorsal surface covered with cortex, they make up the majority of the discoidal backed flakes in the assemblage (n = 51; 72.86 %). This reduction in the predominance of non-cortical

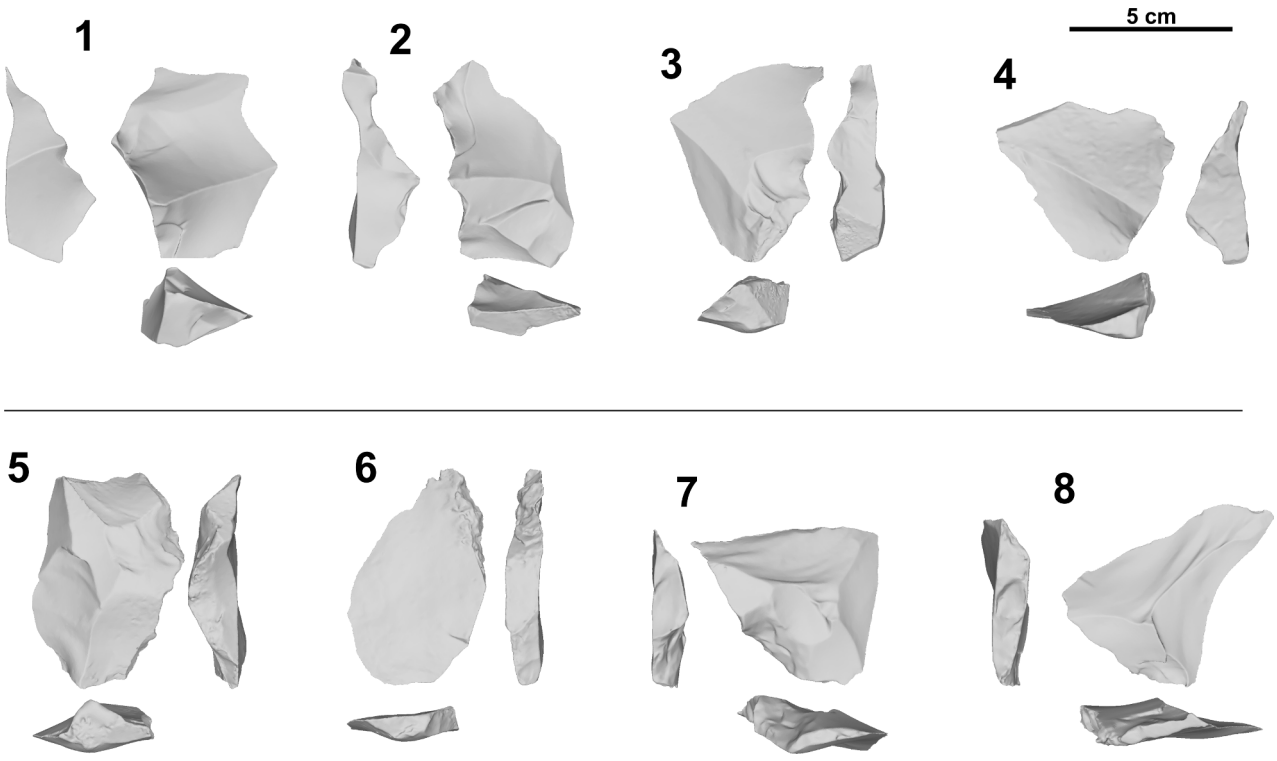

Fig. 3. Backed products from the experimental sample: core edge flakes (1–2) and pseudo-Levallois points (3–4) from the Discoid knapping method. Core edge flakes (5–6) and pseudo-Levallois points (7–8) from the Levallois recurrent centripetal method.

flakes is also expected in discoidal methods given the organization of both debitage surfaces, the nature of the surface convexities, and the fracture plane. In discoidal cores, the interchangeable surfaces usually have a higher apical convexity than Levallois cores. Additionally, the angle and removal of flakes cover a smaller portion of the respective surface than in a Levallois core. Thus, it is expected that as reduction continues, some products will retain a certain amount of cortex.

2.2. Data acquisition

All flakes were scanned with an Academia 20 structured light surface scanner (Creaform 3D) at a 0.2 mm resolution. Flakes were scanned in two parts and automatically aligned (or manually aligned in case automatic alignment failed) and exported in STL formats. Cloudcompare 2.11.3 (https://www.danielgm.net/cc/) free software was employed to perform additional cleaning, mesh sampling, surface reconstruction, and transformation into PLY files. Finally, all files were decimated to a quality of 50,000 faces using the Rvcg R package v.0.21 (Schlager, 2017).

The protocol for the digitalization of landmarks on flakes was based on previous studies (Archer et al., 2021, 2018). This included the positioning of a total of 3 fixed landmarks, 85 curve semi-landmarks, and 420 surface semi-landmarks (Bookstein, 1997a, 1997b; Gunz et al., 2005; Gunz and Mitteroecker, 2013; Mitteroecker and Gunz, 2009). This makes for a total of 508 landmarks and semi-landmarks. The three fixed landmarks correspond to both laterals of the platform width, and the percussion point. The 85 curve semi-landmarks correspond to the internal and exterior curve outlines of the platform (15 semi-landmarks each) and the edge of the flake (55 semi-landmarks), and the 60 surface semi-landmarks correspond to the platform surface. The dorsal and ventral surfaces are defined by 180 semi-landmarks each. The workflow for digitalizing the landmarks and semi-landmarks included the creation of a template/atlas on an arbitrary selected flake (Fig. 5, top). After this, the landmarks and semi-landmarks were positioned in each specimen and were relaxed to minimize bending energy (Fig. 5, bottom; Bookstein, 1997a, b). The entire workflow of landmark and semi-landmarks digitalization and relaxation to minimize bending energy was done in Viewbox version 4.1.0.12 (https://www.dhal.com/viewbox.htm), and resulting point coordinates were exported into.xlsx files.

Procrustes superimposition (Kendall, 1984; Mitteroecker and Gunz, 2009; O'Higgins, 2000) was performed using the package "Morpho" v.2.9 (Schlager, 2017) on RStudio IDE (R Core Team, 2019; RStudio Team, 2019). After performing Procrustes superimposition and obtaining a new set of coordinates, PCA was performed to reduce the dimensionality of the data (James et al., 2013; Pearson, 1901). There are multiple reasons to use dimensionality reduction when dealing with high dimensional data on classification, including to avoid having more predictors than observations ($p > n$), to avoid the collinearity of predictors, to reduce the dimensions of the feature space, and to avoid overfitting due to an excessive number of degrees of freedom (simple structure with lower number of variables). PCA achieves dimensionality reduction by identifying the linear combinations that best represent the predictors in an unsupervised manner. The principal components (PCs) of a PCA are aimed to capture as high a variance as possible of the complete data (James et al., 2013), and PCs that capture a higher variance do not necessarily need to be the best for classification. For the present work, PCs that represent 95 % of the variance were selected as predictors for training the machine learning models. The threshold of 95 % of the variance was arbitrarily selected since it balances retaining most of the dataset variance on a reduced number of variables. The identification of best PCs for classification was automatically done by the machine learning models using the caret v.6.0.92 package (Kuhn, 2008).

A drawback exists in the interpretability of PCA as a result of its nature of reducing dimensionality through the identification of linear combinations of variables. Because of this, interpreting what morphological features are being capture by a PC can be difficult. An option for interpreting PC is to use manual measurements as predictive variables on multiple linear regressions to predict PC values. In addition to

geometric morphometrics, the following attributes were recorded for each of the flakes using the E5 software (McPherron, 2019).

- **Technological length:** measured in mm along the axis perpendicular to the striking platform.
- **Technological width:** measured in mm along the axis perpendicular to the technological length.
- **Maximum thickness** of the flake measured in mm.
- **External platform angle (EPA):** measured in degrees with a manual goniometer.
- **Internal platform angle (IPA):** measured in degrees with a manual goniometer.
- **Relative amount of cortex on the dorsal face:** recorded according to its extension on the dorsal surface of the flake, with categories as follows: 0 (no cortex), 1 (nearly 25 % covered by cortex), 2 (nearly 50 % covered by cortex), 3 (nearly 75 % covered by cortex), and 4 (nearly the entire surface covered by cortex). This variable was employed to evaluate the distribution of cortex proportions among the experimental assemblage (Fig. 4).
- **Weight:** measured to a precision of 0.01 g.

These measures served to generate the following indices:

- **Elongation index:** length divided by width.
- **Carenation index:** result of dividing either width or length (the one with the lowest value) between maximum thickness.
- **Width to thickness ratio:** flake width divided by maximum thickness.

These measures are not employed as inputs for the Machine Learning models, but to explore the meaning of the Principal Components through multiple linear regression.

2.3. Machine learning models and evaluation

The following 11 machine learning models have been tested for differentiating between backed flakes extracted from the two surfaces of the core within each knapping method:

- **Linear discriminant analysis (LDA):** reduces dimensionality aiming to maximize the separation between classes while decision boundaries divide the predictor range into regions (Fisher, 1936; James et al., 2013).
- **K-nearest neighbor (KNN):** classifies cases by assigning the class of similar known cases. The "k" in KNN references the number of cases (neighbors) to consider when assigning a class, and it must be found by testing different values. Given that KNN uses distance metrics to compute nearest neighbors and that each variable is in different scales, it is necessary to scale and center the data prior to fitting the model (Cover and Hart, 1967; Lantz, 2019).
- **Logistic regression:** essentially adapts continuous regression predictions to categorical outcomes (Cramer, 2004; Walker and Duncan, 1967).
- **Decision tree with C5.0** algorithm: is an improvement on decision trees for classification (Quinlan, 2014, 1996).
- **Random forest:** is made of decision trees. Each tree is grown from a random sample of the data and variables, allowing for each tree to grow differently and to better reflect the complexity of the data (Breiman, 2001).
- **Gradiant Boosting Machine** (Greenwell et al., 2019; Ridgeway, 2007) implements gradient boosted (Friedman, 2002, 2001), allowing the detection of learning deficiencies and increases model accuracy.
- **Supported vector machine (SVM):** fits hyperplanes into a multidimensional space with the objective of creating homogeneous partitions (Cortes and Vapnik, 1995; Frey and Slate, 1991). The present study tests SVM with linear, radial, and polynomial kernels.
- **Artificial neural network (ANN):** with multi-layer perception, uses a series of hidden layers and error backpropagation for model training (Rumelhart et al., 1986).
- **Naïve Bayes:** computes class probabilities using Bayes' rule (Weihs et al., 2005).

All models are evaluated using 10 × 50 k-fold cross validation (10 folds and 50 cycles), providing measures of accuracy. Using a 10-fold division, each fold will have 14 data points (with the exception of the last fold, which will have 13 data points). Each fold serves subsequently as test set for a trained model. Although computationally more expensive, this guarantees that all data points will serve as test sets. The 50 cycles provide a random shuffling of the dataset prior to fold division, thus ensuring that the composition of the folds varies in each cycle and it does not play a significant role in the evaluation of the models.

Machine Learning models commonly use a 0.5 classification threshold to assign categories. However, classification thresholds can be modified to balance the ability of model to detect true positives and avoid false positives which are respectively referred as sensitivity and specificity (this problem is exemplified in Fig. 6). The receiver operating characteristic (ROC) curve is employed to systematically evaluate the ratio of detected true positives while avoiding false positives (Bradley, 1997; Spackman, 1989). The ROC curve allows visually analyzing model performance and calculating the AUC, which ranges from 1 (perfect classifier) to 0.5 (random classifier). AUC ranges of values are usually

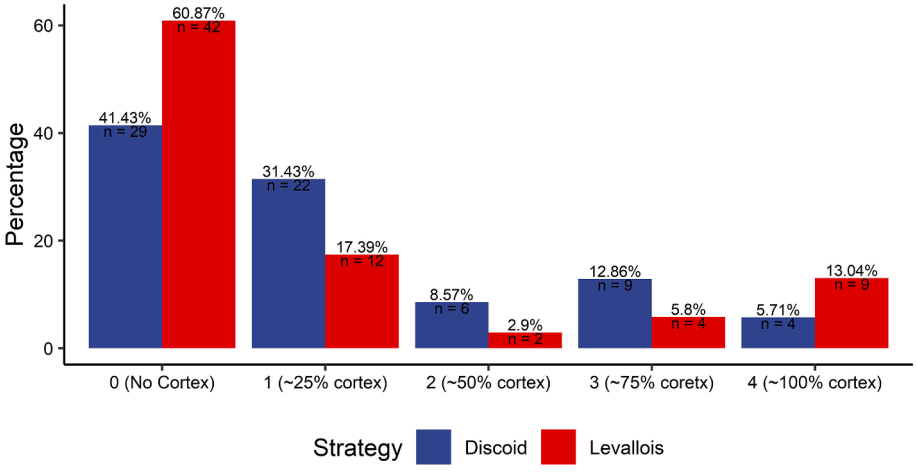

Fig. 4. Distribution of backed flakes according to the relative cortex amount for both strategies.

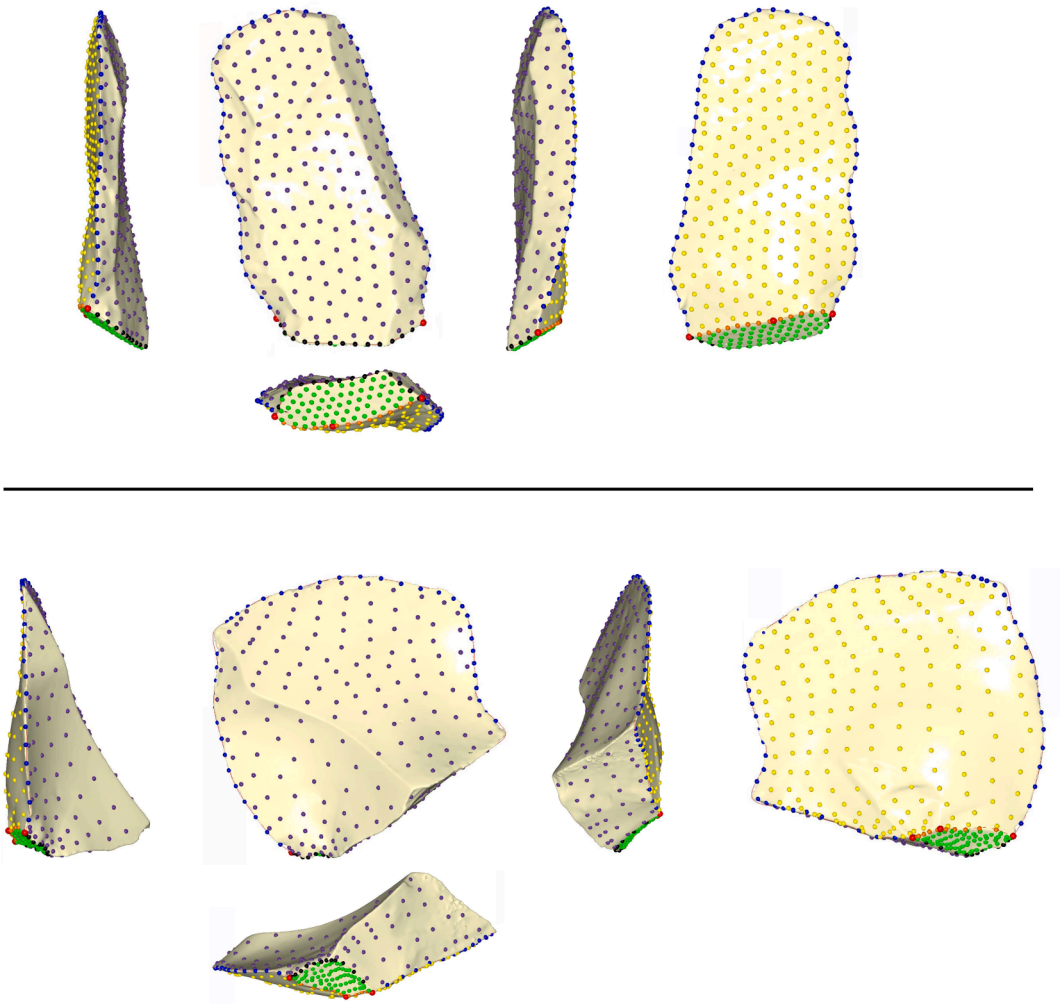

Fig. 5. Top: Template/atlas on an arbitrary selected flake with the defined landmarks (in red), curves, and surfaces. Bottom: Landmark positioning after sliding to minimize bending energy on a pseudo-Levallois point from a discoidal reduction sequence.

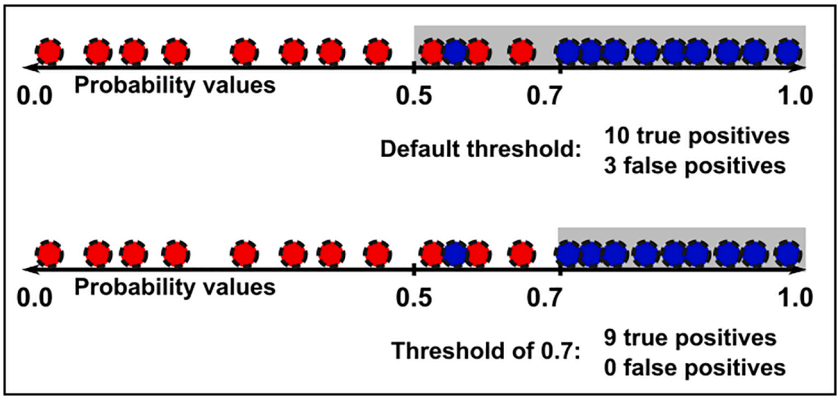

Fig. 6. Examples of the use of different thresholds for classification. The upper example uses a default threshold of 0.5 for classification. The lower example uses a 0.7 threshold avoiding three false positives at the expense of one true positive.

interpreted as follows: 1 to 0.9: outstanding; 0.9 to 0.8: excellent/good; 0.8 to 0.7: acceptable/fair; 0.7 to 0.6: poor; and 0.6 to 0.5: no discrimination (Lantz, 2019). When analyzing lithic assemblages, the use of thresholds to guarantee true positives and avoid false positives is of special interest. The use of decision thresholds and derived measures of accuracy (ROC curve and AUC) can be especially useful in lithic analysis since it is expected that products from initial reduction stages are morphologically similar, independent of the knapping method. It is expected that these products show a higher mixture between methods and have lower probability values. The use of thresholds better indicates the accuracy of a model since it takes into account these probability values.

Statistical analysis was carried out using R version 4.1.2 in IDE RStudio version 2021.09.0 (R Core Team, 2019; RStudio Team, 2019). The management of the data and the generation of graphs was done

using the tidyverse v.1.3.1 package (Wickham et al., 2019). The training of LDA and KNN was done with MASS v.7.3.57 (Venables and Ripley, 2002). The training of random forest was done using the "ranger" v.0.13.1 package (Wright and Ziegler, 2017). The training of SVM was done using the e1071 v.1.7.9 package (Karatzoglou et al., 2006, 2004). The RSNNS v.0.4.14 (Bergmeir and Benítez, 2012) package was employed to train multi-layer ANN with backpropagation. The klaR v.1.7.0 package was employed to train the naive Bayes classifier (Weihs et al., 2005). The k-fold cross validation of all models, precision metrics, and confusion matrix were obtained using the caret v.6.0.92 package (Kuhn, 2008). Machine learning models also provide insights into the variable importance for classification. The caret package was employed to extract variable importance after each k-fold cross validation. Package pROC v.1.18.0 is employed to obtain ROC curve and AUC data.

All 3D models, original coordinates, data, code, models and complete workflow is freely available at the corresponding Zenodo repository (https://doi.org/10.5281/zenodo.7085139).

3. Results

3.1. PCA and model performance

The PCA results (Fig. 7) show that the first 25 PCs account for 95 % of the variance of the dataset, with PC1 accounting for 21.39 % of the variance and PC25 accounting for 0.36 % of the variance. This is an important reduction from the original number of variables (1,524) and is substantially lower than the sample (1 3 9).

Fig. 8 presents the performance metrics for each of the models. In general, all models performed with accuracy values higher than 0.7 with the exception of KNN, Naïve Bayes, and the decision tree with C5.0 algorithm. When considering the two measures of overall model performance (F1 and accuracy), SVM with polynomial kernel presents the highest performance values (F1 = 0.75 and accuracy = 0.757). Additionally, SVM with polynomial kernel also provides the highest values of precision.

SVM with polynomial kernel is closely followed by SVM with a linear kernel, which presents the second highest value of accuracy (0.741), the fourth highest value of F1 (0.726), and the second-highest value of precision (0.774). Outside SVM with different kernels, the boosted trees also presents high values of accuracy (0.732), F1 (0.732), and precision (0.738). KNN presented the lowest values on the general performance metrics, with an accuracy value of 0.61 and a very low F1 score (0.461). KNN does seem to present high values of precision (0.751) and specificity (0.888) although these are clearly the result of a sensitivity (0.333) lower than the no-information ratio (0.504).

The evaluation of the models through the ROC curve and AUC (Fig. 9) shows that most models present acceptable/fair (0.8–0.7) values. Again, KNN presents the lowest AUC (0.67), a poor value. SVM with polynomial kernel presents the highest AUC value (0.799) and is thus very close to being an excellent/good model (0.9 to 0.8). The optimal probability threshold values from the SVM with polynomial kernel are 0.501 for discoidal and 0.491 for Levallois. The general performance metrics (F1 and accuracy) and AUC values indicate that SVM with polynomial kernel is the best model. The evaluation of SVM with the polynomial kernel confusion matrix (Fig. 10) shows a very good distribution along the diagonal axis, with the correct identification of Levallois products being slightly higher than the correct identification of discoidal products. The directionality of confusions shows that for the SVM with polynomial kernel, it is more common to mistake discoidal backed products for Levallois ones rather than mistaking Levallois backed products for those from discoidal reduction sequences.

3.2. Feature importance

Fig. 11 presents the PC importance for the discrimination of knapping method according to SVM with polynomial kernel model. The PC importance shows that PC3 clearly stands out in importance for the discrimination of discoidal and Levallois backed products. PC3 only accounts for 10.8 % of the variance but presents the maximum scaled importance. PC1, which represents 21.39 % of the variance, is the second most important variable, with a score of 46.64, although far from PC3. PC8, which represents only 3.63 % of the variance, is the third most important variable for the SVM with polynomial kernel model.

The effect of PC3 on identifying backed products from the two

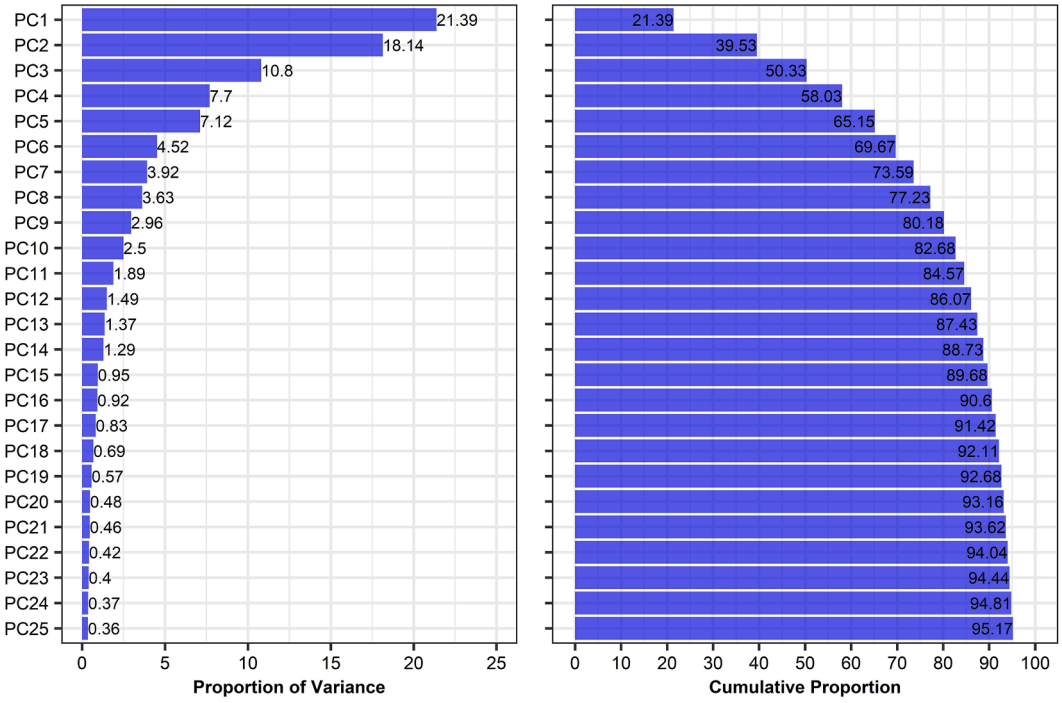

Fig. 7. Proportion of variance and cumulative proportion of the first 25 PC.

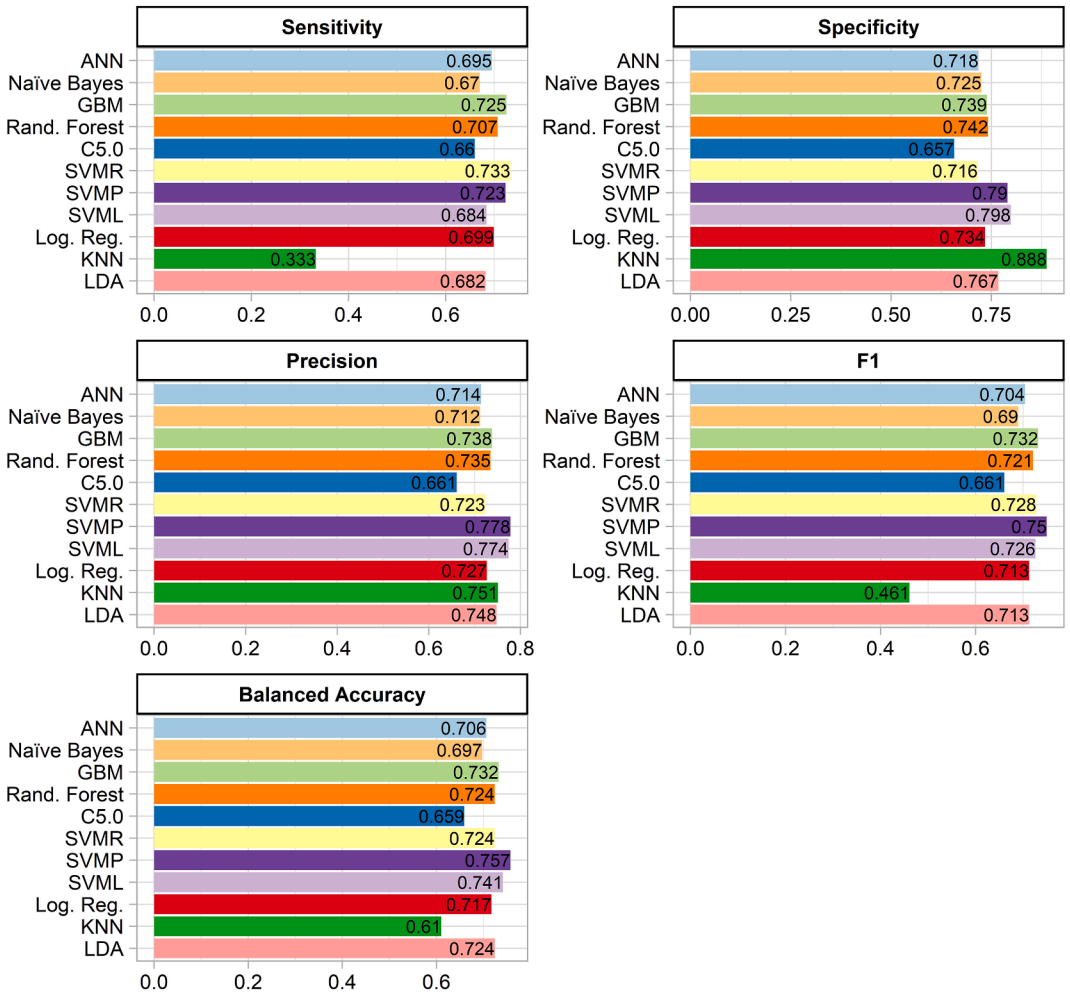

Fig. 8. Performance metrics of models.

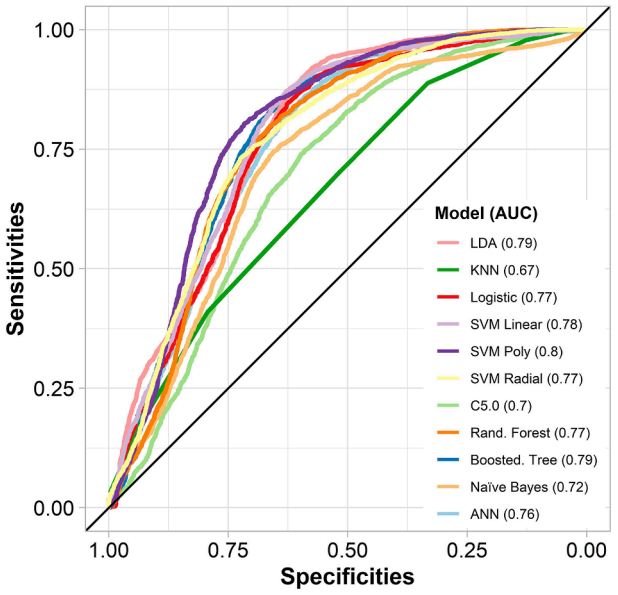

Fig. 9. ROC curves and AUC values of each of the tested models.

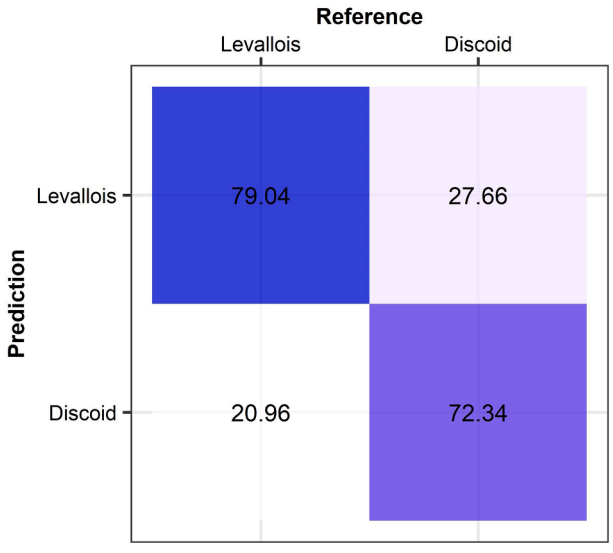

Fig. 10. Normalized confusion matrix of SVM with polynomial kernel. Top left represents percentage of backed flakes from Levallois recurrent centripetal correctly identified as belonging to that strategy. Bottom left represents percentage of backed flakes from Levallois recurrent centripetal incorrectly identified as belonging to discoidal reduction sequences.

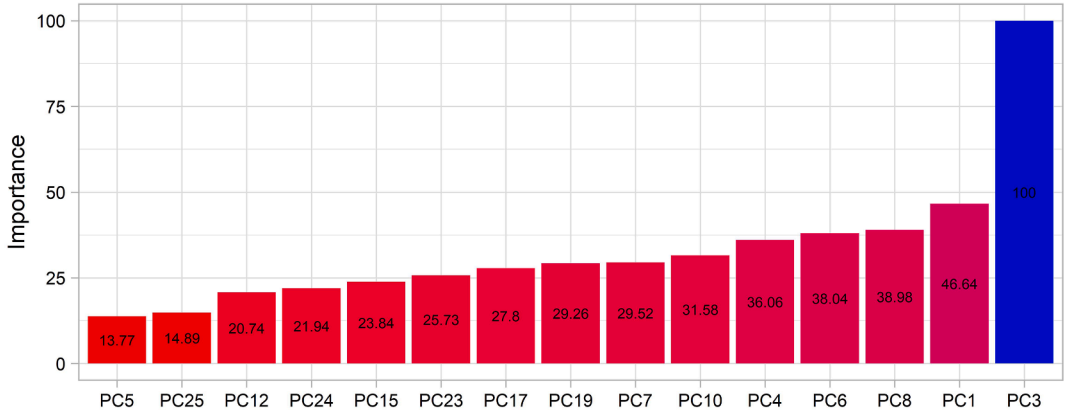

Fig. 11. Variable importance of each of the PCs for SVM with polynomial kernel model.

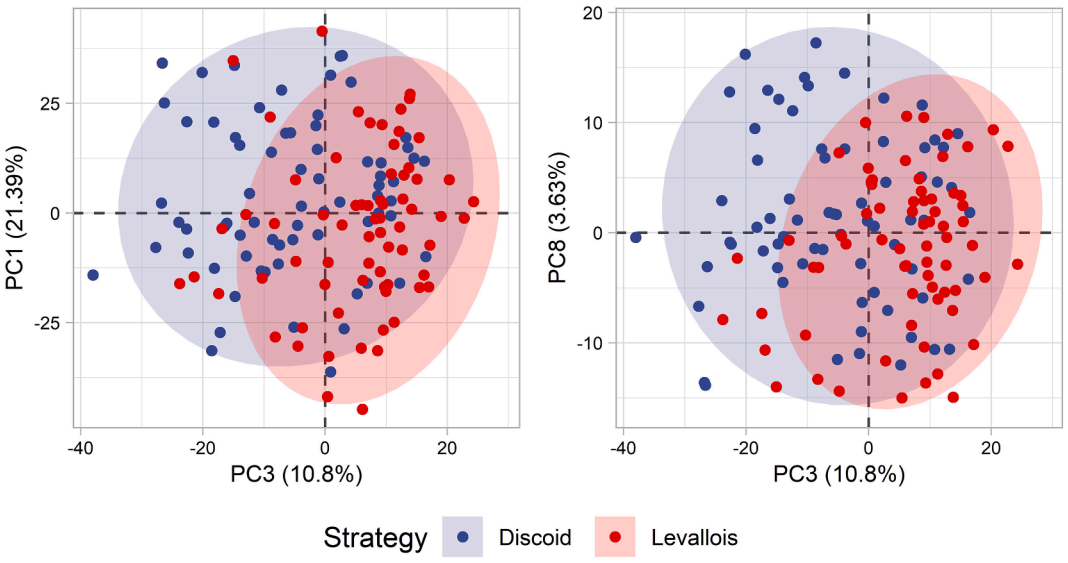

Fig. 12. Biplots of PC3, PC1, and PC8 (and percentage of variance explained) according to their importance in the SVM with polynomial kernel model.

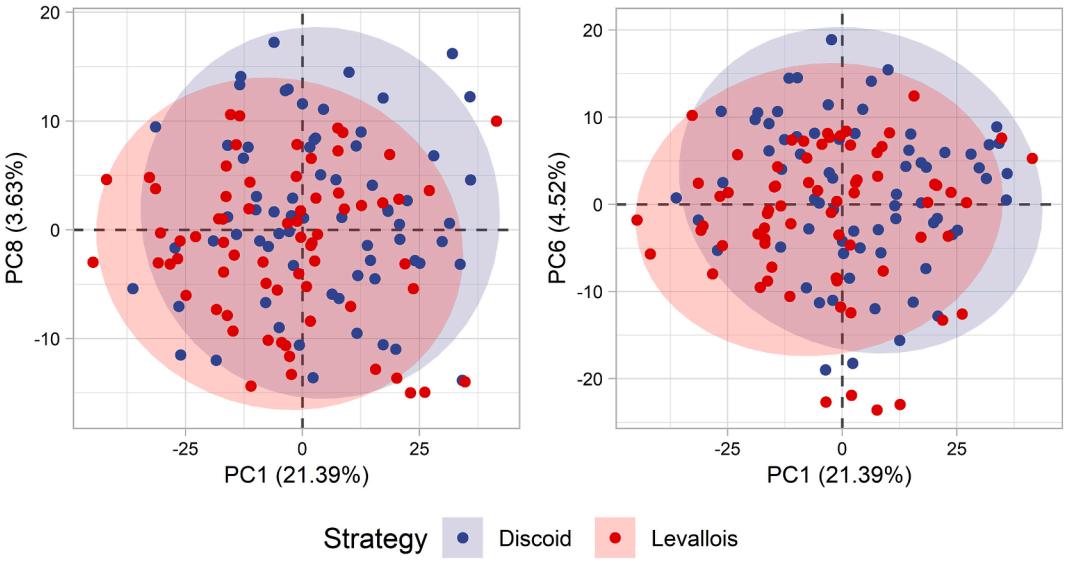

Fig. 13. Biplots of PC1, PC6, and PC8 (and percentage of variance explained) according to their importance in the SVM with polynomial kernel model.

knapping methods is especially notable in the a biplot distribution. Fig. 12 presents a biplot distribution of the data between PC3 and the following two most important variables. In both cases, backed flakes detached from Levallois recurrent centripetal cores tend to be clustered in the positive values of PC3, whereas they show a wider distribution, usually centered on the 0 value, for PCs 1 and 8. Backed flakes from discoidal reduction sequences show a wider distribution although the center is in the negative and 0 values of PC3. Although the combination of PC3 with PC1 and PC8 shows an overlapping of the confidence ellipsis, differentiation between both groups can be observed.

Fig. 13 presents a biplot distribution of the data when the second (PC1), third (PC8), and fourth (PC6) most important variables are employed. The biplot from the combination of these variables (Fig. 13) shows much more consistent overlapping for the different combinations of PC1, PC8, and PC6.

3.3. Multiple linear regression and feature interpretation

Multiple linear regression for the prediction of PC3 indicates that the best correlation is obtained when the interaction of IPA and the ratio of flake width to thickness is employed ($p < 0.001$, adjusted $r^2 = 0.65$). The coefficient of the interaction between the ratio of width to thickness and IPA is 0.17, whereas the coefficient of IPA is −0.77. This indicates that as the IPA becomes more open as the values of PC3 decrease. The ratio of flake width to thickness offers a counterintuitive coefficient of −12.79. The signal of this coefficient is opposite to that obtained from a linear regression where the values of the ratio of flake width to thickness are employed to predict PC3 values ($p < 0.001$; $r^2 = 0.6$; coefficient = 6.46). The reversed signal obtained from the interaction can be considered the result of Simpson's paradox (Simpson, 1951). The high correlation between the carenated index and the ratio of flake width to thickness ($p < 0.001$; $r^2 = 0.9$) indicates that PC3 captures relative flake thinness to thickness although it regresses better with the ratio of width to thickness. In general, thin flakes with an IPA close to 90° will have high positive PC3 values, whereas thick flakes with open IPA will have negative values.

An analysis of PC3 values according to group (Table 1) shows that backed products from Levallois recurrent centripetal methods tend to have higher values (mean = 5.47) with a slightly lower standard deviation. Backed products detached from discoidal cores, alternatively, tend to have lower values (mean = -5.20) and a slightly higher standard deviation (12.74).

Multiple linear regression for the prediction of PC1 values shows a moderate correlation when the elongation index and carenated index are employed as predictors ($p < 0.001$; adjusted $r^2 = 0.63$). The elongation index presents the highest significance and the highest estimate value (-39.27), whereas the carenated index presents an estimate value of −4.26. The negative and high value of the estimate for the elongation index indicates that as the elongation tendency of a product increases (becoming longer relative to its width), the values of PC1 will decrease while all other variables remain constant. The negative estimate of the carenated index also indicates that as a product becomes thinner, the values of PC1 will decrease. Thus, the positive values of PC1 represent thick products with a low elongation.

The analysis of PC1 values shows differences between the backed products of the discoidal and Levallois recurrent centripetal methods. On average, backed products from the Levallois recurrent centripetal method will have higher values (mean = 3.75) compared to discoidal products (mean = -3.80). However, an important overlapping of values is evident for products from both reduction methods, with high values of standard deviation in both cases.

Table 1
Descriptive statistics of PC3 and PC1 according to knapping method.

	PC3		PC1	
	Discoid	Levallois	Discoid	Levallois
Min	−38.00	−23.82	−36.23	−44.76
5th Percentile	−26.51	−16.16	−26.25	−31.17
1st quantile	−14.74	0.39	−7.71	−16.30
Mean	−5.39	5.47	3.75	−3.80
Median	−5.20	8.59	2.37	−2.74
3rd quantile	4.98	12.41	16.79	7.58
95 Percentile	13.38	18.24	32.96	25.18
Max	16.49	24.29	35.95	41.46
SD	12.74	10.45	17.31	18.11

4. Discussion

Our results have shown an accuracy of 0.76 for the differentiation of backed pieces from discoidal and Levallois recurrent centripetal methods. Additionally, the use of decision thresholds provided an AUC close to 0.8. This degree of accuracy indicates that the quantification of morphological features through geometric morphometrics, along with dimensionality reduction using PCA and machine learning models, can accurately differentiate between the two methods tested. Of the 11 models tested, SVM with polynomial kernel provided the best performance for the discrimination of discoidal and Levallois recurrent centripetal methods in backed artifacts. Moreover, results support the notion that discoidal and recurrent centripetal Levallois are two separate core reduction methods/conceptions.

The selection of machine learning algorithms depends on the task, type of classification, and nature of the data, requiring for the systematical evaluation of different algorithms. Of the tested models, SVM with polynomial kernel performed the best. SVM's have a series of features which make them ideal for the analysis of lithic artifacts. As previously mentioned, SVM models fit hyperplanes to separate classes, use margins to find the best separation, and apply a cost value with each misclassification (Lantz, 2019). Selection of the kernel is key for the performance of SVM, since it will have a direct impact on the fitted hyperplane, margins and cost value. As a result of these features, SVM are able to allow misclassifications and overlapping classifications in order to obtain a better general performance. These features of SVM make them especially adequate for the analysis of lithic materials and might be one of the underlying reasons why it has the best performance metrics.

The first 25 PCs captured 95 % of the sample variance. Of these PCs, the highest importance value for the discrimination of knapping methods was obtained by PC3. Multiple linear regression shows that PC3 is moderately correlated with an interaction between IPA and the ratio of flake width to thickness. Thin and wide artifacts with IPA values close to 90° will have higher PC3 values. The examination of biplots and PC3 values shows that backed flakes detached from Levallois recurrent centripetal cores tend to be thin in relation to the thickness, non-elongated, and have an IPA close to 90°. PC1, which captures elongation tendencies with higher resolution (along with product thickness) also supports this interpretation although higher overlapping exists. The discriminatory power of PC3 appears inherently related to differences in how the volume of cores in the two methods are conceived: non-hierarchized surfaces exploited with secant removals in discoidal reduction while recurrent centripetal Levallois is characterized by sub-parallel removals from a single debitage surface. Additional features for the discrimination of discoidal and Levallois backed products can be found in edge angles and the angles of negatives of the dorsal face towards the detachment surface. In general, it is expected that products detached from Levallois reduction sequences will have more acute edge angles, along with flatter dorsal surface negatives. Again, these differences in the angles are also inherently related to differences in how the volume of cores in the two methods are conceived.

These results indicate that there are underlying morphological differences between backed artifacts detached from both methods. These underlying morphological differences can be captured and quantified by geometric morphometrics along with PCA and used by machine learning models for an accurate discrimination of methods.

Several authors have identified underlying morphological characteristics that can differentiate backed products detached from Levallois recurrent centripetal and discoidal cores (Boëda et al., 1990; Delpiano et al., 2021; Meignen, 1993, 1996; Mourre, 2003). As previously suggested, one of the features captured by PC3 is the internal platform angle (IPA). Products with an IPA close to 90° have increasing PC3 values, which is the case for most backed flakes from Levallois reduction sequences. Levallois products having an IPA close to 90° was identified relatively early on (Kelly, 1954) and further documented following the detailed technological description of the Levallois flaking system (Boëda, 1993, 1994, 1995a,b). A recent study employing machine learning models (González-Molina et al., 2020) based on an attribute analysis have also pointed to the IPA as one of the features differentiating Levallois recurrent centripetal and Discoid products.

Delpiano et al., (2021) focused on the general morphology of backed products from discoidal and Levallois reduction sequences, stating that the latter tend to be thinner with subparallel and rectilinear edges and a higher elongation index. The interpretation of PC3 in the present study also identifies backed products from Levallois recurrent centripetal as being thinner. However, the interpretation of PC1 (which better captures elongation) proved not to be a sound criterion for discriminating between strategies, with both methods showing a very wide range of elongation values. Concerning the elongation of Levallois products, Boëda et al. (1990) also noticed the decrease of length/width ratio with each successive exploitation phase, resulting in short non-laminar flakes and core edge flakes. Mourre (2003) equally called attention to the direction of removal axis being parallel to the plane of intersection of both surfaces in the case of Levallois core edge flakes. In our study, the effect of this feature can be linked to a higher carenation index, which is captured by PC3. The visual exploration of the 3D meshes according to PC values did not seem to capture the relation between the debitage axis and the symmetry of blanks as an important feature of Levallois centripetal backed flakes (Meignen, 1993, 1996). This is probably due to the inclusion of core edge flakes with a limited back in the experimental sample and its possible importance being overshadowed by other features better for discrimination captured by PC3 (IPA, carenation index and elongation index).

González-Molina et al., (2020) achieved an 80 % accuracy when differentiating between discoidal and Levallois centripetal flakes. Although their study focused uniquely on flakes from the exploitation phase (with the presence of cortex having very little importance as a variable for differentiating methods), it did not specifically addressed the issue of backed flakes, and dimensional variables (width at different points and maximum thickness) have high importance, it shows the potential of using machine learning models for the identification of knapping methods. In contrast, our study focused on a concrete set of technological products independent of the reduction phase, and the use of geometric morphometrics excludes dimensional variables. However, despite these differences, similar degrees of accuracy were obtained. Archer et al., (2021) also used geometric morphometrics and random forest to evaluate the differentiation between three strategies (Levallois, discoidal, and laminar). Although overall performance of the models is based on accuracy, their study nevertheless reached a similar value to that of the present study. However, the classification of the two same classes as in the present study varies significantly, with an 87 % accuracy for Levallois products and 40 % in the differentiation of discoidal products. This contrasts heavily with our results, where the classification is more balanced and the identification of backed products from discoidal reduction showed a slightly lower accuracy than the identification of products from the Levallois recurrent centripetal method (0.72 and 0.79, respectively).

Archer et al., (2021) also reported human analyst identification ratios for flakes from different archaeological sites with the "undiagnostic" class being the largest, usually tallying above 60 % (thus, only 35 % of flakes were attributed to a knapping method). In both the above-mentioned studies (Archer et al., 2021; González-Molina et al., 2020) and in the present study, the application of machine learning models notably increases the accuracy and predictions regarding the identification of knapping methods. Caution is always advisable when evaluating such findings, as controlled experimental assemblages do not mimic the complexity of the archaeological record.

The present study has employed multiple linear regression with common metrics of lithic analysis as predictors to determine what features were captured by the PCs. The multiple linear regressions of both PC3 and PC1 presented moderate correlation values, with more than 0.6 of the variance explained. However, this also implies that a good portion of the variance remains unexplained for both PCs. The remaining unexplained variance can be the result of several factors. Metric variables used as predictors were taken manually, likely resulting in some degree of error. Geometric morphometrics capture the same metric variables with higher resolution, thus representing another potential source of error when establishing correlations. An additional source of the unexplained PC variance might come from metric features (and their interactions) recorded as part of exhaustive attribute analyses (e.g. the number, organization and flaking angle of previous removals). This suggests future research should take into account large sample sizes along with the incorporation of these analytical features.

While backed flakes detached from discoidal and Levallois recurrent centripetal methods were the focus of our analysis, it is important to note that backed products are common to other flaking strategies such as Quina and SSDA (Bourguignon, 1996; Forestier, 1993) not included in the present study. Although in Western Europe the coexistence of Levallois and discoidal knapping methods with other knapping methods in the same archaeological levels is a subject of debate (Faivre et al., 2017; Grimaldi and Santaniello, 2014; Marciani et al., 2020; Ríos-Garaizar, 2017), the present model can be applied to assemblages where Levallois and Discoid knapping strategies have been shown to coexist. For this, the study and evaluation of the *chaîne opèratoire* and assemblage context and integrity are fundamental for the study of lithic technology (Soressi and Geneste, 2011). Thus, the *chaîne opèratoire* and assemblage integrity should be considered prior to the application of geometric morphometrics and machine learning models for the identification of knapping methods.

5. Conclusions

Backed flakes are technological products that play special roles in the discoidal and Levallois recurrent centripetal methods (Boëda, 1993; Boëda et al., 1990; Slimak, 2003). In Levallois reductions, these removals serve to manage lateral and distal core convexities (Boëda et al., 1990), while their systematic production in discoidal reductions demonstrates their properties to be intentionally sought-after (Locht, 2003; Slimak, 2003). Additionally, data from several sites show that they were commonly imported and exported (Geneste, 1988; Roebroeks et al., 1992; Turq et al., 2013, Courbin et al. 2020). This frequent transport is possibly connected to their specific morpho-functional features (Delpiano et al., 2021), a "prehensile" core edge opposite a convergent cutting edge. Associated with two technologically distinct core reduction methods, it should be expected that their morphological features differ and therefore allow for the identification of the knapping method. With the use of geometric morphometrics, these morphological features can be quantified, and PCA for dimensionality reduction allows them to be employed in machine learning models.

PCA and machine learning models indeed capture the different morphological features derived from both knapping methods, resulting in an accuracy of 0.76 and an AUC of 0.8 in the case of the best model for differentiating between knapping strategies. Most of the importance for differentiating between the knapping methods was captured by only one variable (PC3), which multiple linear regressions showed to be correlated with the elongation index and mostly an interaction between IPA and the carenation index.

The workflow of the present work has been developed to allow for its

implementation on archaeological materials. Archaeological backed flakes can be scanned, then use the flake template from the present work to locate landmarks on the 3D meshes, perform procrustes alignment of all backed flakes (archaeological and experimental reference flakes of the present research whose original unaligned coordinates are available), reduce dimensionality of experimental and archaeological backed flakes through PCA (it is important to notice that PCA values will change with the inclusion of new archaeological data), train the SVM with polynomial kernel on the experimental assemblage, and make predictions on the archaeological material. Of this workflow, 3D scanning and landmarks positioning are considered to be the most time-consuming stages, while procrustes alignment, PCA and model training can be considered to be fairly fast.

Geometric morphometrics in combination with dimensionality reduction methods (PCA) and machine learning models can offer high-resolution methods for the identification of knapping methods in lithic analysis although their application should not be independent from the study of the operative chain and assemblage technological context.

Author contributions

GBP: conceptualization, data curation, formal analysis, resources, investigation, methodology, writing original draft. MB and BG: resources, validation, draft review and editing. FR: conceptualization, resources, methodology, funding acquisition, project administration, supervision, and draft review and editing.

Declaration of Competing Interest

The authors declare that they have no known competing financial interests or personal relationships that could have appeared to influence the work reported in this paper.

Data availability

Data available at Zenodo

Acknowledgments

The authors wish to thank the co-editor and the two anonymous reviewers for their comments and suggestions. This research has been supported by the project SI1/PJI/2019-00488 funded by Comunidad Autónoma de Madrid and Universidad Autónoma de Madrid. FR research studies are also supported by the project ID2019-103987GB-C33 funded by the Spanish Ministry of Science and Innovation.

Appendix A. Supplementary material

Supplementary data to this article can be found online at https://doi.org/10.1016/j.jasrep.2022.103723.

References

Archer, W., Pop, C.M., Rezek, Z., Schlager, S., Lin, S.C., Weiss, M., Dogandžić, T., Desta, D., McPherron, S.P., 2018. A geometric morphometric relationship predicts stone flake shape and size variability. Archaeological and Anthropological Sciences 10, 1991–2003. https://doi.org/10.1007/s12520-017-0517-2.

Archer, W., Djakovic, I., Brenet, M., Bourguignon, L., Presnyakova, D., Schlager, S., Soressi, M., McPherron, S.P., 2021. Quantifying differences in hominin flaking technologies with 3D shape analysis. J. Hum. Evol. 150, 102912 https://doi.org/10.1016/j.jhevol.2020.102912.

Beyries, S., Boëda, E., 1983. Étude technoloogique et traces d'utilisation des éclats débordants de Corbehem (Pas-de-Calais). Bulletin de la Société préhistorique française 80, 275–279. https://doi.org/10.3406/bspf.1983.5455.

Binford, L.R., 1979. Organization and Formation Processes: Looking at Curated Technologies. J. Anthropol. Res. 35, 255–273.

Boëda, E., 1993. Le débitage discoïde et le débitage Levallois récurrent centripède. Bulletin de la Société Préhistorique Française 90, 392–404. https://doi.org/10.3406/bspf.1993.9669.

Boëda, E., 1994. Le concept Levallois: variabilité des méthodes. CNRS, CNRS éditions.

Boëda, E., 1995a. Caractéristiques techniques des chaînes opératoires lithiques des niveaux micoquiens de Külna (Tchécoslovaquie). Paléo 1, 57–72. https://doi.org/10.3406/pal.1995.1380.

Boëda, E., 1995b. Levallois: A Volumetric Construction, Methods, A Technique. In: Dibble, H.L., Bar-Yosef, O. (Eds.), The Definition and interpretation of Levallois Technology, Monographs in World Archaeology. Prehistory Press, Madison, Wisconsin, pp. 41–68.

Boëda, E., Geneste, J.-M., Meignen, L., 1990. Identification de chaînes opératoires lithiques du Paléolithique ancien et moyen. Paléo 2, 43–80.

Bookstein, F.L., 1997a. Morphometric tools for landmark data. Cambridge University Press.

Bookstein, F.L., 1997b. Landmark methods for forms without landmarks: morphometrics of group differences in outline shape. Med. Image Anal. 1, 225–243. https://doi.org/10.1016/S1361-8415(97)85012-8.

Bordes, F., 1953. Notules de typologie paléolithique II : Pointes Levalloisiennes et pointes pseudo-levalloisiennes. bspf 50, 311–313. https://doi.org/10.3406/bspf.1953.3057.

Bordes, F., 1961. Typologie du Paléolithique ancien et moyen, Publications de l'institut de préhistoire de l'université de Bordeaux. CNRS Editions, Bordeaux.

Bourguignon, L., 1996. La conception du debitage Quina. Quaternaria Nova 6, 149–166.

Bourguignon, L., Turq, A., 2003. Une chaîne opératoire de débitage discoïde sur éclat du Moustérien à denticulés aquitain: les exemples de Champ Bossuet et de Combre Grenal c.14, in: Peresani, M. (Ed.), Discoid Lithic Technology. Advances and Implications, BAR International Series. Oxford, pp. 131–152.

Bradley, A.P., 1997. The use of the area under the ROC curve in the evaluation of machine learning algorithms. Pattern Recogn. 30, 1145–1159.

Breiman, L., 2001. Random Forests. Machine Learning 45, 5–32. https://doi.org/10.1023/A:1010933404324.

Brenet, M., Cretin, C., 2008. Le gisement paléolithique moyen et supérieur de Combemenue (Brignac-la-plaine, Corrèze). Du microvestige au territoire, réflections sur les perspectives d'une approche multiscalaire, in: Aubry, T., Almeida, F., Araújo, A.C., Tiffagom, M. (Eds.), Proceedings of the XV World Congress UISPP (Lisbon, 4-9 September 2006). Space and Time: Which Diachronies, Which Synchronies, Which Scales? / Typology vs Technology, Sessions C64 and C65, BAR International Series. Archaeopress, Oxford, pp. 35–44.

Brenet, M., 2012. Silex et roches métamorphiques au Paléolithique moyen récent: Combemenue (Corrèze) et Chemin d'Herbe (Lot-et-Garonne), in: Marchand, G., Querré, G. (Eds.), Roches et Sociétés de La Préhistoire Entre Massifs Cristallins et Bassins Sédimentaires : Le Nord-Ouest de La France Dans Son Contexte Européen. Presses universitaires de Rennes, pp. 379–393.

Brenet, M., 2013. Variabilité et signification des productions lithiques au Paléolithique moyen ancien. L'exemple de trois gisements de plein-air du Bergeracois (Dordogne, France), BAR International Series. Archaeopress, Oxford.

Bustillo, M.A., Pérez-Jiménez, J.L., 2005. Características diferenciales y génesis de los niveles silíceos explotados en el yacimiento arqueológico de Casa Montero (Vicálvaro, Madrid). Geogaceta 38, 243–246.

Bustillo, M.Á., Pérez-Jiménez, J.L., Bustillo, M., 2012. Caracterización geoquímica de rocas sedimentarias formadas por silicificación como fuentes de suministro de utensilios líticos (Mioceno, cuenca de Madrid). Revista Mexicana de Ciencias Geológicas 29, 233–247.

Bustos-Pérez, G., Chacón, M.G., Rivals, F., Blasco, R., Rosell, J., 2017. Quantitative and qualitative analysis for the study of Middle Paleolithic retouched artifacts: Unit III of Teixoneres cave (Barcelona, Spain). J. Archaeolog. Sci.: Rep. 12, 658–672. https://doi.org/10.1016/j.jasrep.2017.02.021.

Cortes, C., Vapnik, V., 1995. Support-vector networks. Machine learning 20, 273–297.

Courbin, P., Brenet, M., Michel, A., Gravina, B., 2020. Spatial analysis of the late Middle Palaeolithic open-air site of Bout-des-Vergnes (Bergerac, Dordogne) based on lithic technology and refitting. J. Archaeolog. Sci.: Rep. 32, 102373 https://doi.org/10.1016/j.jasrep.2020.102373.

Cover, T., Hart, P., 1967. Nearest neighbor pattern classification. IEEE Trans. Inform. Theory 13, 21–27. https://doi.org/10.1109/TIT.1967.1053964.

Cramer, J.S., 2004. The early origins of the logit model. Studies in History and Philosophy of Science Part C: Studies in History and Philosophy of Biological and Biomedical Sciences 35, 613–626. https://doi.org/10.1016/j.shpsc.2004.09.003.

Delagnes, A., 1995. Variability within Uniformity: Three Levels of Variability within the Levallois System. In: Dibble, H.L., Bar-Yosef, O. (Eds.), The Definition and interpretation of Levallois Technology, Monographs in World Archaeology. Prehistory Press, Madison, Wisconsin, pp. 201–211.

Delagnes, A., Meignen, L., 2006. Diversity of Lithic Production Systems During the Middle Paleolithic in France. Are There Any Chronological Trends? In: Hovers, E., Kuhn, S.L. (Eds.), Transitions Before the Transition Evolution and Stability in the Middle Paleolithic and Middle Stone Age. Springer, pp. 85–107.

Delpiano, D., Gennai, J., Peresani, M., 2021. Techno-Functional Implication on the Production of Discoid and Levallois Backed Implements. Lithic Technology 46, 171–191. https://doi.org/10.1080/01977261.2021.1886487.

Duran, J.-P., 2005. L'industrie moustérienne des Ànecs (Rodès, Pyrénées-orientales, France). PYRENAE 36, 11–39.

Duran, J.-P., Soler, N., 2006. Variabilité des modalités de débitage et des productions lithiques dans les industries moustériennes de la grotte de l'Arbreda, secteur alpha (Serinyà, Espagne). Bulletin de la Société Préhistorique Française 103, 241–262.

Faivre, J.-P., Gravina, B., Bourguignon, L., Discamps, E., Turq, A., 2017. Late Middle Palaeolithic lithic technocomplexes (MIS 5–3) in the northeastern Aquitaine Basin: Advances and challenges. Quat. Int. 433, 116–131. https://doi.org/10.1016/j.quaint.2016.02.060.

Fernandes, P., Morala, A., Schmidt, P., Séronie-Vivien, M.-R., Turq, A., 2012. Le silex du Bergeracois: état de la question. Quaternaire Continental d'Aquitaine, excursion AFEQ, ASF 2012 (2012), 22–33.

Fisher, R.A., 1936. The use of multiple measurements in taxonomic problems. Ann. Eugen. 7, 179–188.
Folgado, M., Brenet, M., 2010. Economie de débitage et organisation de l'espace technique sur le site du Paléolithique moyen de plein-air de La Mouline (Dordogne, France). In: Conard, N., Delagnes, A. (Eds.), Settlement Dynamics of the Middle Paleolithic and Middle Stone Age. Kerns Verlag - (Tübingen Publications in Prehistory), Tübingen, pp. 427–454.
Forestier, H., 1993. Le Clactonien: mise en application d'une nouvelle méthode de débitage s'inscrivant dans la variabilité des systèmes de production lithique du Paléolithique ancien. pal 5, 53–82. https://doi.org/10.3406/pal.1993.1104.
Frey, P.W., Slate, D.J., 1991. Letter recognition using Holland-style adaptive classifiers. Machine learning 6, 161–182.
Geneste, J.-M., 1988. Les Industries De La Grotte Vaufrey: Technologie du debitage, economie et circulation de la matiere premiere lithique. In: Rigaud, J.-.-P. (Ed.), La Grotte Vaufrey À Cenac Et Saint-Julien (Dordogne): Paléoenvironnements, Chronologie Et Activités Humaines, Mémoires De La Société Préhistorique Française (Revue). Société préhistorique française, Paris, pp. 441–517.
González-Molina, I., Jiménez-García, B., Maíllo-Fernández, J.-M., Baquedano, E., Domínguez-Rodrigo, M., 2020. Distinguishing Discoid and Centripetal Levallois methods through machine learning. PLoS ONE 15, e0244288.
Grimaldi, S., Santaniello, F., 2014. New insights into Final Mousterian lithic production in western Italy. Quat. Int. 350, 116–129. https://doi.org/10.1016/j.quaint.2014.03.057.
Gunz, P., Mitteroecker, P., Bookstein, F.L., 2005. Semilandmarks in three dimensions. In: Modern Morphometrics in Physical Anthropology. Springer, New York, pp. 73–98.
Gunz, P., Mitteroecker, P., 2013. Semilandmarks: a method for quantifying curves and surfaces. Hystrix 24, 103–109. https://doi.org/10.4404/hystrix-24.1-6292.
James, G., Witten, D., Hastie, T., Tibshirani, R., 2013. An Introduction to Statistical Learning with Applications in R, Second Edition. ed. Springer.
Karatzoglou, A., Smola, A., Hornik, K., Zeileis, A., 2004. kernlab - An S4 Package for Kernel Methods in R. J. Stat. Softw. 11, 1–20. https://doi.org/10.18637/jss.v011.i09.
Karatzoglou, A., Meyer, D., Hornik, K., 2006. Support Vector Machines in R. J. Stat. Softw. 15, 1–28. https://doi.org/10.18637/jss.v015.i09.
Kelly, H., 1954. Contribution à l'étude de la technique de la taille levalloisienne. Bulletin de la Société Préhistorique Française 51, 149–169. https://doi.org/10.3406/bspf.1954.3077.
Kendall, D.G., 1984. Shape Manifolds, Procrustean Metrics, and Complex Projective Spaces. Bull. London Math. Soc. 16, 81–121. https://doi.org/10.1112/blms/16.2.81.
Kuhn, M., 2008. Building Predictive Models in R using the caret Package. J. Stat. Softw. 28 https://doi.org/10.18637/jss.v028.i05.
Kuhn, S.L., 2013. Roots of the Middle Paleolithic in Eurasia. Current Anthropology 54. https://doi.org/10.1086/673529.
Lantz, B., 2019. Machine learning with R: expert techniques for predictive modeling. Packt publishing ltd.
Lenoir, M., Turq, A., 1995. Recurrent Centripetal Debitage (Levallois and Discoidal): Continuity or Discontinuity? In: Dibble, H.L., Bar-Yosef, O. (Eds.), The Definition and interpretation of Levallois Technology, Monographs in World Archaeology. Prehistory Press, Madison, Wisconsin, pp. 249–256.
Locht, J.-L., 2003. L'industrie lithique du gisement de Beauvais (Oise, France): objectifs et variabilité du débitage discoïde. In: Peresani, M. (Ed.), Discoid Lithic Technology: Advances and Implications, BAR International Series. Archaeopress, Oxford, pp. 193–209.
Marciani, G., Ronchitelli, A., Arrighi, S., Badino, F., Bortolini, E., Boscato, P., Boschin, F., Crezzini, J., Delpiano, D., Falcucci, A., Figus, C., Lugli, F., Oxilia, G., Romandini, M., Riel-Salvatore, J., Negrino, F., Peresani, M., Spinapolice, E.E., Moroni, A., Benazzi, S., 2020. Lithic techno-complexes in Italy from 50 to 39 thousand years BP: An overview of lithic technological changes across the Middle-Upper Palaeolithic boundary. Quat. Int. 551, 123–149. https://doi.org/10.1016/j.quaint.2019.11.005.
Martín-Viveros, J.I., Ollé, A., Chacón, M.G., Romagnoli, F., Gómez de Soler, B., Vaquero, M., Saladié, P., Vallverdú, J., Carbonell, E., 2020. Use-wear analysis of a specific mobile toolkit from the Middle Paleolithic site of Abric Romaní (Barcelona, Spain): a case study from level M. Archaeol. Anthropol. Sci. 12, 16. https://doi.org/10.1007/s12520-019-00951-z.
McPherron, S., 2019. E5 (Beta Version), Source code.
Meignen, L., 1996. Persistance des traditions techniques dans l'abri des Canalettes (Nant-Aveyron). Quaternaria Nova 6, 449–464.
Meignen, L., 1993. Les industries lithiques de l'abri des Canalettes: cuche 2, in: Meignen, L. (Ed.), L'abri des Canalettes. Un habitat moustérien sur les grands Causses (Nant-Aveyron), Monographie du CRA. CNRS Ed., Paris, pp. 238–328.
Mitteroecker, P., Gunz, P., 2009. Advances in Geometric Morphometrics. Evol. Biol. 36, 235–247. https://doi.org/10.1007/s11692-009-9055-x.
Mourre, V., 2003. Discoïde ou pas Discoïde? Réflexions sur la pertinence des critères techniques définissant le débitage discoïde, in: Peresani, M. (Ed.), Discoid Lithic Technology. Advances and Implications, BAR International Series. Archaeopress, Oxford, pp. 1–17.
O'Higgins, P., 2000. The study of morphological variation in the hominid fossil record: biology, landmarks and geometry. J. Anat. 197, 103–120. https://doi.org/10.1046/j.1469-7580.2000.19710103.x.
Pasty, J.-F., Liegard, S., Alix, P., 2004. Étude de l'industrie lithique du site paléolithique moyen des Fendeux (Coulanges, Allier). bspf 101, 5–25. https://doi.org/10.3406/bspf.2004.12945.
Pearson, K., 1901. On lines and planes of closest fit to systems of points in space. The London, Edinburgh, and Dublin Philosophical Magazine and Journal of Science 2, 559–572. https://doi.org/10.1080/14786440109462720.
Picin, A., Chacón, M.G., Gómez de Soler, B., Blasco, R., Rivals, F., Rosell, J., 2020. Neanderthal mobile toolkit in short-term occupations at Teixoneres Cave (Moia, Spain). J. Archaeolog. Sci.: Rep. 29, 102165 https://doi.org/10.1016/j.jasrep.2019.102165.
Quinlan, J.R., 1996. Improved Use of Continuous Attributes in C4.5. jair 4, 77–90. https://doi.org/10.1613/jair.279.
Quinlan, J.R., 2014. C4. 5: programs for machine learning. Elsevier.
R Core Team, 2019. R: A language and environment for statistical computing. R Foundation for Statistical Computing, Vienna, Austria.
Ríos-Garaizar, J., 2017. A new chronological and technological synthesis for Late Middle Paleolithic of the Eastern Cantabrian Region. Quat. Int. 433, 50–63. https://doi.org/10.1016/j.quaint.2016.02.020.
Roebroeks, W., Loecker, D.D., Hennekens, P., Leperen, M.V., 1992. "A veil of stones": on the interpretation of an early Middle Palaeolithic low density scatter at Maastricht-Belvédère (The Netherlands). Analecta Praehistorica Leidensia 25| The end of our third decade: Papers written on the occasion of the 30th anniversary of the Institutte of prehistory, volume I 25, 1–16.
Romagnoli, F., Trenti, F., Nannini, L., Carmignani, L., Ricci, G., Lo Vetro, D., Martini, F., Sarti, L., 2016a. Raw material procurement and productive sequences in the Palaeolithic of southern Italy: the Tyrrhenian and the Ionian areas. Ressources lithiques, productions et transferts entre Alpes et Méditerranée 185–205.
Romagnoli, F., Bargalló, A., Chacón, M.G., Gómez de Soler, B., Vaquero, M., 2016b. Testing a hypothesis about the importance of the quality of raw material on technological changes at Abric Romaní (Capellades, Spain): Some considerations using a high-resolution techno-economic perspective. JLS 3, 635–659. https://doi.org/10.2218/jls.v3i2.1443.
RStudio Team, 2019. RStudio: Integrated Development for R. RStudio, Inc., Boston, MA.
Rumelhart, D.E., Hinton, G.E., Williams, R.J., 1986. Learning representations by back-propagating errors. Nature 323, 533–536.
Schlager, S., 2017. Morpho and Rvcg-Shape Analysis in R: R-Packages for geometric morphometrics, shape analysis and surface manipulations. Statistical Shape and Deformation Analysis. Elsevier 217–256.
Shott, M.J., 2018. The Costs and Benefits of Technological Organization: Hunter-Gatherer Lithic Industries and Beyond. In: Robinson, E., Sellet, F. (Eds.), Lithic Technological Organization and Paleoenvironmental Change. Springer International Publishing, Cham, pp. 321–333. https://doi.org/10.1007/978-3-319-64407-3_15.
Simpson, E.H., 1951. The Interpretation of Interaction in Contingency Tables. J. Roy. Stat. Soc.: Ser. B (Methodol.) 13, 238–241. https://doi.org/10.1111/j.2517-6161.1951.tb00088.x.
Slimak, L., 2003. Les Debitages discoïdes mousteriens: evaluation d'un concept technologique. In: Peresani, M. (Ed.), Discoid Lithic Technology. Advances and Implications, BAR International Series. Archaeopress, Oxford, pp. 33–65.
Soressi, M., Geneste, J.-M., 2011. The History and Efficacy of the Chaîne Opératoire Approach to Lithic Analysis: Studying Techniques to Reveal Past Societies in an Evolutionary Perspective. PaleoAnthropology 2011, 334–350. https://doi.org/10.4207/PA.2011.ART63.
Spackman, K.A., 1989. Signal detection theory: Valuable tools for evaluating inductive learning, in: Proceedings of the Sixth International Workshop on Machine Learning. Elsevier, pp. 160–163.
Terradas, X., 2003. Discoid flaking method: conception and technological variability, in: Peresani, M. (Ed.), Discoid Lithic Technology. Advances and Implications, BAR International Series. Archaeopress, Oxford, pp. 19–32.
Turq, A., Roebroeks, W., Bourguignon, L., Faivre, G.-P., 2013. The fragmented character of Middle Palaeolithic stone tool technology. J. Hum. Evol. 65, 641–655. https://doi.org/10.1016/j.jhevol.2013.07.014.
Venables, W.N., Ripley, B.D., 2002. Modern applied statistics with S, Fourth, Edition. ed. Statistics and Computing, Springer, New York.
Walker, S.H., Duncan, D.B., 1967. Estimation of the Probability of an Event as a Function of Several Independent Variables. Biometrika 54, 167–179. https://doi.org/10.2307/2333860.
Weihs, C., Ligges, U., Luebke, K., Raabe, N., 2005. klaR analyzing German business cycles. Data Anal. Decis. Support. Springer 335–343.
Wickham, H., Averick, M., Bryan, J., Chang, W., McGowan, L., François, R., Grolemund, G., Hayes, A., Henry, L., Hester, J., Kuhn, M., Pedersen, T., Miller, E., Bache, S., Müller, K., Ooms, J., Robinson, D., Seidel, D., Spinu, V., Takahashi, K., Vaughan, D., Wilke, C., Woo, K., Yutani, H., 2019. Welcome to the Tidyverse. J. Open Source Softw. 4, 1686. https://doi.org/10.21105/joss.01686.
Wright, M.N., Ziegler, A., 2017. ranger: A Fast Implementation of Random Forests for High Dimensional Data in C++ and R. J. Stat. Softw. 77, 1–17. https://doi.org/10.18637/jss.v077.i01.